Modular and Global Sparse Synchronization in Clustered Small-World Networks of Inhibitory Fast Spiking Izhikevich Interneurons

Sang-Yoon Kim and Woochang Lim
Institute for Computational Neuroscience and Department of Science Education,
Daegu National University of Education, S. Korea

Introduction

- **Fast Sparsely Synchronized Brain Rhythms**
  - Population level: Fast oscillations [e.g. gamma rhythm (30~100Hz) and sharp-wave ripple (100~200Hz)]
  - Cellular level: Stochastic and intermittent discharges
  - Associated with diverse cognitive functions [e.g., sensory perception, feature integration, selective attention, and memory formation and consolidation]
- **Modular Architecture of Real Brain**
  - Modular structure of brain: The mammalian brain (e.g., cat and macaque) has been revealed to have a modular structure composed of sparsely linked clustered with spatial localization.
  - Complex topology in modules: Connection architecture of the real brain reveals complex topology such as small-worldness and scale-freeness which are neither regular nor random.
  - Our neuronal model: Clustered Small-World Network (SWN)
- **Purpose of Our Study**
  Investigation of Effect of Intermodular Synaptic Connections on Emergence of Sparsely Synchronized Brain Rhythms in Clustered SWN

Clustered Small-World Networks

- **Clustered Networks with M Small-World (SW) Sub-Networks**

Intra-modular connection: Small-World Network
Inter-modular connection: Random

M: No. of Sub-Networks (M=3)
Each Cluster: Small-World Sub-Network
Composed of L Inhibitory Fast Spiking (FS) Izhikevich Interneurons
Izhikevich Interneuron: not only biologically plausible (Hodgkin-Huxley neuron-like), but also computationally efficient (IF neuron-like)

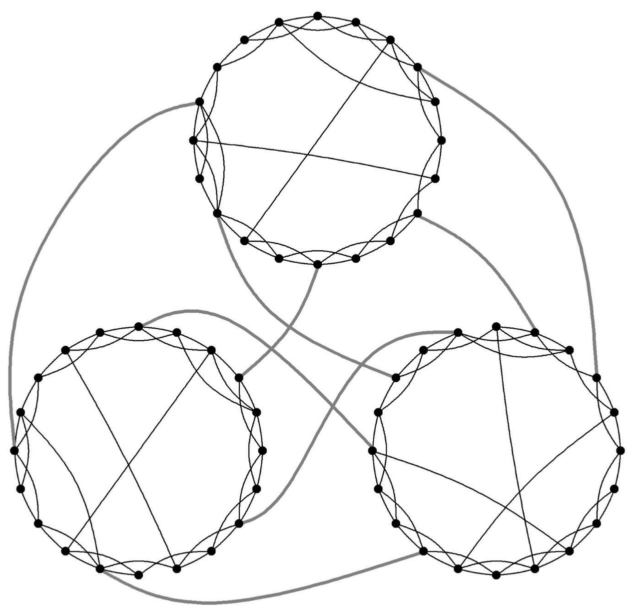

Fast Sparsely Synchronized Rhythms in SW Sub-Networks

- **Intra-Modular Dynamics**
  Fast Sparsely Synchronized State with the population frequency f_p=147 Hz and the individual neuron's mean firing rate f_i=33 Hz.

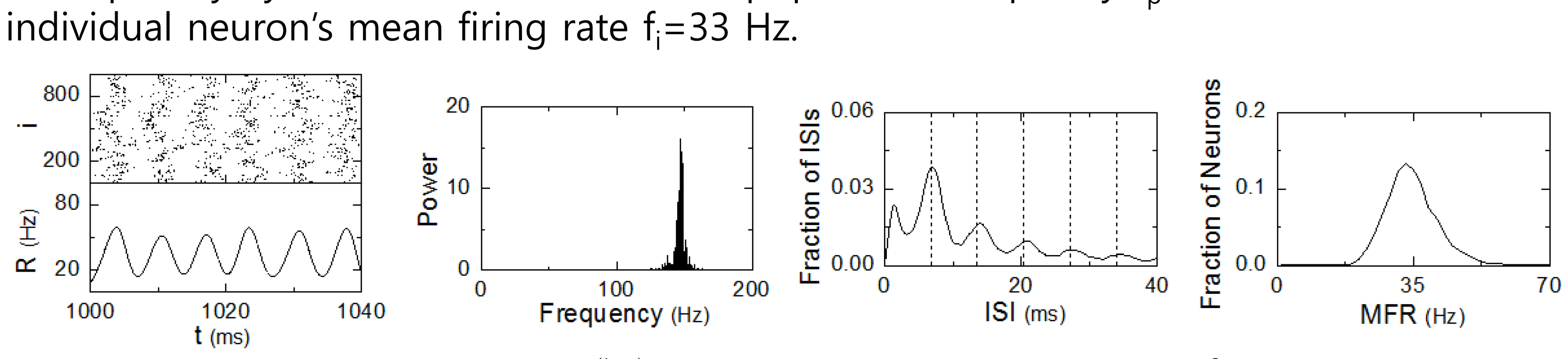

$I_{DC}=1500, M_{syn}^{(intra)}=50, J_{intra}=1400, D=500, p_{rewiring}=0.25, L=10^3$

Modular and Global Synchronization in Clustered SWN

$M=3, M_{syn}^{(inter)}=20$

- **Instantaneous Population Spike Rate**
  Instantaneous sub-population spike rate for the Ith sub-network:

$$R_s^{(I)}(t)\equiv\frac{1}{L}\sum_{i=1}^{L}\sum_{s=1}^{n_i^{(I)}}K_h(t-t_s^{(I,i)})$$

$t_s^{(I,i)}$: sth spiking time of the ith neuron in the Ith sub-network
$n_i^{(I)}$: Total number of spikes for the ith neuron in the Ith sub-network

Gaussian kernel function of band width h:

$$K_h(t)=\frac{1}{\sqrt{2\pi}h}e^{-t^2/2h^2},\quad -\infty<t<\infty$$

Instantaneous whole-population spike rate for the whole network:

$$R_w(t)\equiv\frac{1}{M}\sum_{I=1}^{M}R_s^{(I)}(t)$$

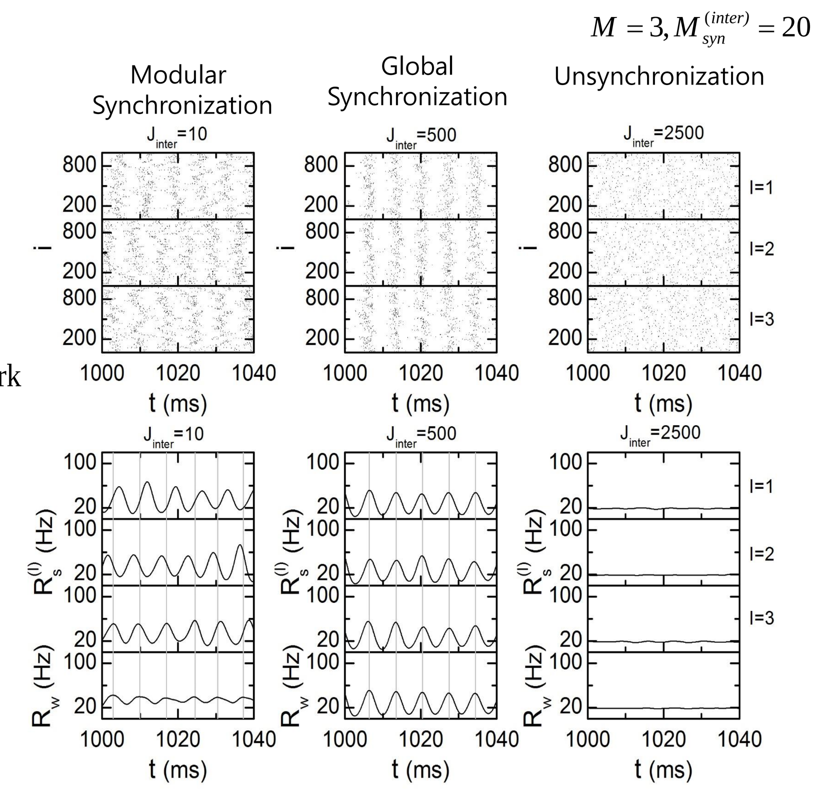

- **State Diagram in the $J_{inter}-M_{syn}^{(inter)}$ Plane**

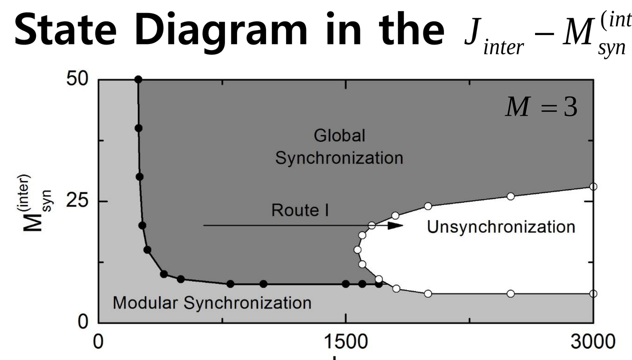

Modular Synchronization: Mismatching between intra-modular dynamics of sub-networks
Global Synchronization: Matching between intra-modular dynamics of sub-networks

Synchronization-Unsynchronization Transition (Route I with $M_{syn}^{(inter)}=20$)

- **Realistic Thermodynamic Order Parameter**
  Sub-population order parameter for the Ith sub-network:

$$\mathcal{O}_s^{(I)}\equiv\overline{(R_s^{(I)}(t)-\overline{R_s^{(I)}(t)})^2}\qquad(I=1,2,3)$$

Overbar represents the time average.

Whole-population order parameter for the whole network:

$$\mathcal{O}_w\equiv\overline{(R_w(t)-\overline{R_w(t)})^2}$$

For the synchronized (unsynchronized) state, $\mathcal{O}_s^{(I)}$ and $\mathcal{O}_w$ approach non-zero (zero) limit values in the thermodynamic limit of L→∞.

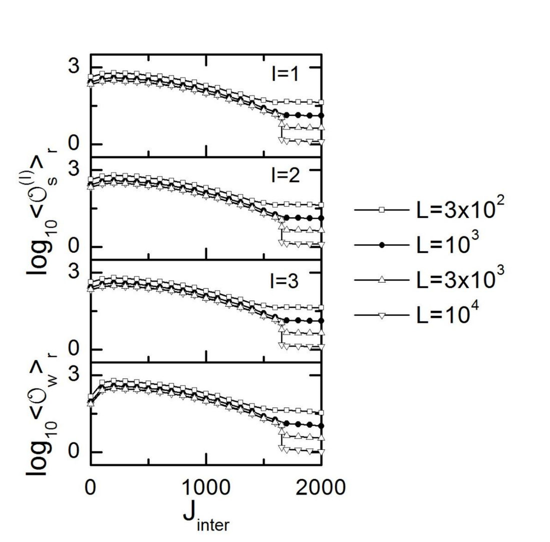

When passing the threshold $J_{inter,h}^{*}(\simeq 1657)$, a transition to unsynchronization occurs.

Synchronized State
Sparse stripes are formed in the raster plot
$R_s^{(I)}(t)$ and $R_w(t)$ show regular oscillations

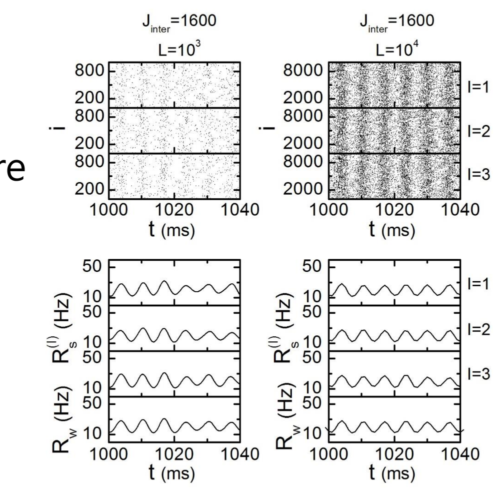

Unsynchronized State
Sparse spikes are scattered in the raster plot
$R_s^{(I)}(t)$ and $R_w(t)$ becomes nearly stationary

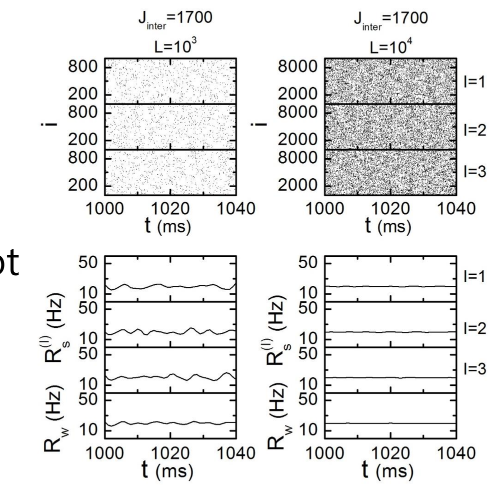

Characterization of Sync. and Unsync. Using the Spatial Cross-correlation (Route I with $M_{syn}^{(inter)}=20$)

- **Spatial Cross-Correlation**
  Instantaneous individual spike rate of the ith neuron in the Ith sub-network: $r_i^{(I)}(t)\equiv\sum_{s=1}^{n_i^{(I)}}K_h(t-t_s^{(I,i)})$

Normalized temporal cross-correlation function between in the instantaneous individual spike rates of the (i, j) neuronal pair in the Ith sub-network:

$$C_{i,j}^{(I)}(\tau)=\frac{\overline{\Delta r_i^{(I)}(t+\tau)\cdot\Delta r_j^{(I)}(t)}}{\sqrt{\overline{\Delta r_i^{(I)2}(t)}}\sqrt{\overline{\Delta r_j^{(I)2}(t)}}},\qquad \Delta r_i^{(I)}(t)=r_i^{(I)}(t)-\overline{r_i^{(I)}(t)}$$

Spatial cross-correlation function: $C_l^{(I)}=\frac{1}{L}\sum_{i=1}^{L}C_{i,i+l}^{(I)}(0)$ for $l=1,\ldots,L/2$.

For synchronized state:
$C_l^{(I)}$: nearly non-zero constant for whole range of l.
Correlation length = L/2
For unsynchronized state:
$C_l^{(I)}$: nearly zero for whole range of l.
Correlation length = 0

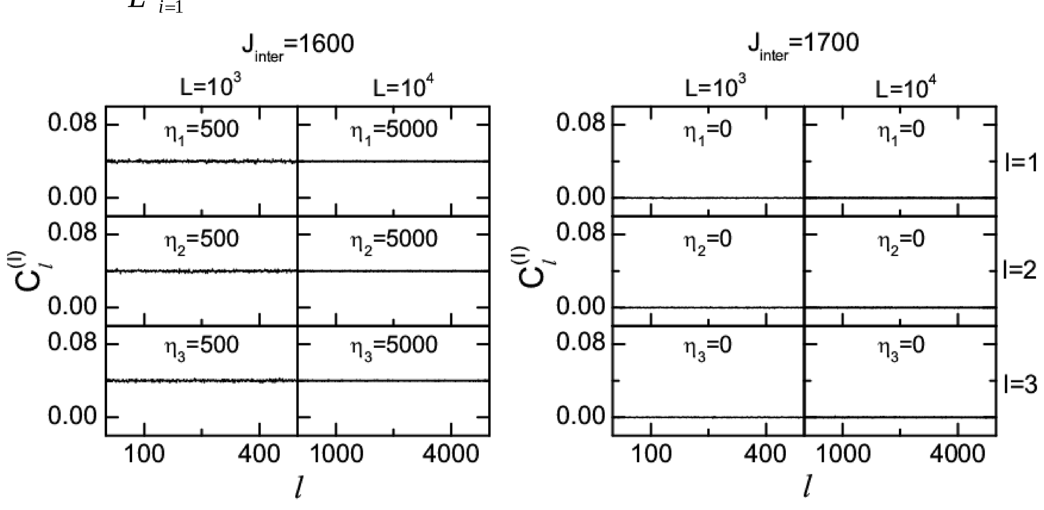

Modular-Global Synchronization Transition (Route I with $M_{syn}^{(inter)}=20$)

- **Modular and Global Synchronization**

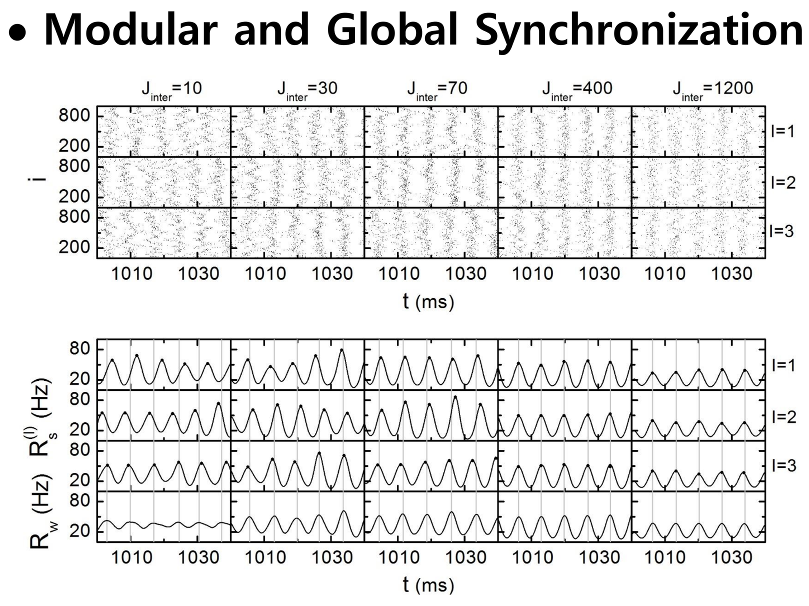

Normalized temporal cross-correlation function between the instantaneous sub-population spike rates:

$$C_{I,J}(\tau)=\frac{\overline{\Delta R_s^{(I)}(t+\tau)\cdot\Delta R_s^{(J)}(t)}}{\sqrt{\overline{\Delta R_s^{(I)2}(t)}}\sqrt{\overline{\Delta R_s^{(J)2}(t)}}}\qquad \Delta R_s^{(I)}(t)=R_s^{(I)}(t)-\overline{R_s^{(I)}(t)}$$

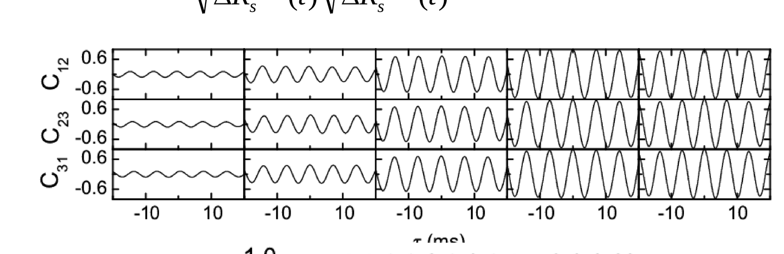

- **Cross-Correlation Modularity Measure**

$$C_M=\frac{2}{M(M-1)}\sum_{I=1}^{M}\sum_{J=I+1}^{M}C_{I,J}(0)$$

$J_{inter}<J_{inter,l}^{*}(\simeq 268)$: Modular Sync. : $0<\langle C_M\rangle_r<1$
$J_{inter,l}^{*}<J_{inter}<J_{inter,h}^{*}$: Global Sync. : $\langle C_M\rangle_r\simeq 1$

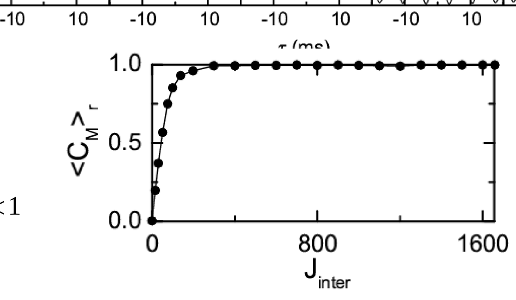

Characterization of Degree of Synchronization (Route I with $M_{syn}^{(inter)}=20$)

- **Realistic Statistical-Mechanical Spiking Measure**
  Occupation degree: representing the density of stripe in the raster plot
  Pacing degree: representing the smearing of stripe in the raster plot (average contribution of all microscopic spikes in the stripe)

With increasing J_{inter},
$\langle O_s^{(I)}\rangle_r$: decreases monotonically.
$\langle P_s^{(I)}\rangle_r$: exhibits the bell-shaped curve.

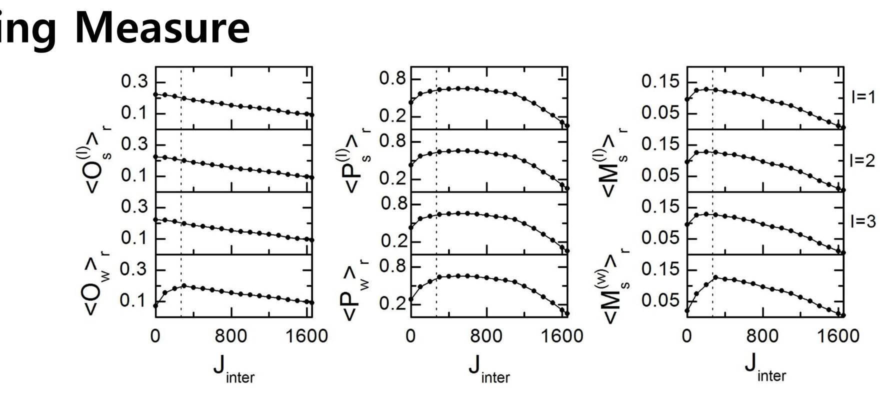

Modular Sync. : $\langle O_s^{(I)}\rangle_r>\langle O_w\rangle_r$, $\langle P_s^{(I)}\rangle_r>\langle P_w\rangle_r$, $\langle M_s^{(I)}\rangle_r>\langle M_s^{(w)}\rangle_r$
Global Sync. : $\langle O_s^{(I)}\rangle_r\simeq\langle O_w\rangle_r$, $\langle P_s^{(I)}\rangle_r\simeq\langle P_w\rangle_r$, $\langle M_s^{(I)}\rangle_r\simeq\langle M_s^{(w)}\rangle_r$

- **Spatial Cross-Correlation Based Measure**
  Subpopulation spatial cross-correlation degree $\langle\langle C_l^{(I)}\rangle_l\rangle_r$: Similar bell-shaped curve
  → The statistical-mechanical pacing degree between spikes seems to be associated with the spatial cross-correlation degree between neuronal pairs.

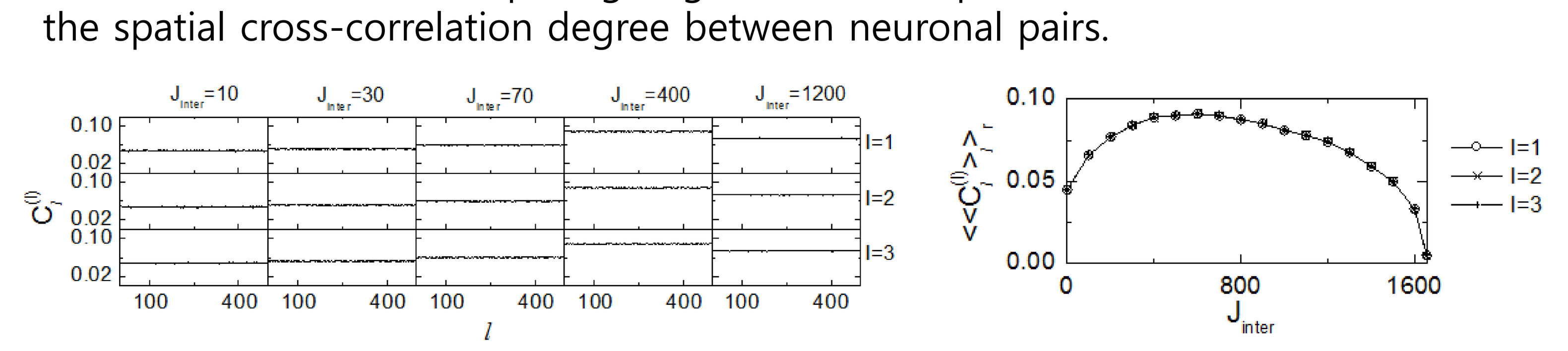

Summary

- **Investigation of The Effect of Inter-Modular Connections on Emergence of Sparsely Synchronized Cortical Rhythms**

Occurrence of Modular Sparse Synchronization and Global Sparse Synchronization Depending on the Values of J_{inter} and $M_{syn}^{(inter)}$

Dual Roles of Inter-Modular Coupling Strength J_{inter} :
For large J_{inter} → Destructive role to "spoil" the pacing between sparse spikings
For small J_{inter} → Constructive role to "favor" the pacing between spikings in each sub-network.

Role of Number of Inter-Modular Connections $M_{syn}^{(inter)}$:
Constructive role to "favor" global communication between sub-networks

Important implications for the role of the **Brain Plasticity** which refers to the brain's ability to change its structure and function by modifying the strength or efficacy of synaptic transmission.